Lipid nanoparticle-mediated codelivery of Cas9 mRNA and single-guide RNA achieves liver-specific in vivo genome editing of *Angptl3*

Min Qiu[a,1], Zachary Glass[a,1], Jinjin Chen[a], Mary Haas[b], Xin Jin[b], Xuewei Zhao[a], Xuehui Rui[a], Zhongfeng Ye[a], Yamin Li[a], Feng Zhang[b], and Qiaobing Xu[a,2]

[a]Department of Biomedical Engineering, Tufts University, Medford, MA 02155; and [b]Broad Institute of MIT and Harvard, Cambridge, MA 02142

Edited by Chad A. Mirkin, Northwestern University, Evanston, IL, and approved January 12, 2021 (received for review September 29, 2020)

Loss-of-function mutations in Angiopoietin-like 3 (*Angptl3*) are associated with lowered blood lipid levels, making *Angptl3* an attractive therapeutic target for the treatment of human lipoprotein metabolism disorders. In this study, we developed a lipid nanoparticle delivery platform carrying Cas9 messenger RNA (mRNA) and guide RNA for CRISPR-Cas9–based genome editing of *Angptl3* in vivo. This system mediated specific and efficient *Angptl3* gene knockdown in the liver of wild-type C57BL/6 mice, resulting in profound reductions in serum ANGPTL3 protein, low density lipoprotein cholesterol, and triglyceride levels. Our delivery platform is significantly more efficient than the FDA-approved MC-3 LNP, the current gold standard. No evidence of off-target mutagenesis was detected at any of the nine top-predicted sites, and no evidence of toxicity was detected in the liver. Importantly, the therapeutic effect of genome editing was stable for at least 100 d after a single dose administration. This study highlights the potential of LNP-mediated delivery as a specific, effective, and safe platform for Cas9-based therapeutics.

lipid nanoparticles | CRISPR-Cas9 mRNA delivery | genome editing | Angptl3

Genome engineering has recently emerged as a potentially powerful therapeutic tool for the treatment of diseases with a genetic etiology. For monogenic disorders, the mutated locus can be directly targeted for repair via genome editing. For complex polygenic disorders such as hyperlipidemia, which are the result of a combination of the effects of a large number of genes as well as nutritional and environmental influences, identifying a single gene to repair may be challenging. An alternative therapeutic approach has been to identify monogenic mutations found naturally in the human population that confer a protection against the disease. By introducing these protective loci, it may be possible to develop a single therapeutic that is effective for many patients, regardless of their specific genetic backgrounds. This strategy has proven successful in the case of *Pcsk9*, wherein loss of function protects against hyperlipidemia: small interfering RNA (siRNA)-mediated *Pcsk9* knockdown strategies have recently completed Phase III clinical trials for the treatment of hyperlipidemia (1, 2).

Angiopoietin-like 3 (ANGPTL3) is an enzyme which regulates plasma lipoprotein levels (3). ANGPTL3 deficiency exists naturally in the human population, resulting from loss-of-function mutations in the *Angptl3* gene (4). These individuals show lowered blood triglycerides (TG) and low-density lipoprotein cholesterol (LDL-C), without any apparent clinical risks or complications resulting from this loss (5, 6). Recent genetic and pharmacologic studies have validated this finding and indicated that *Angptl3* knockdown may confer some protective benefits, making *Angptl3* an attractive therapeutic target for the treatment of human lipoprotein metabolism disorders (7, 8). Two different therapeutic inhibition strategies against ANGPTL3 have recently been validated. In one clinical trial, an ANGPTL3-targeting monoclonal antibody, evinacumab, has proven effective for reducing LDL-C and TG levels in healthy human volunteers (8, 9). These results are in line with a study that found administration of an antisense oligonucleotide (ASO) targeting *Angptl3* messenger RNA (mRNA) achieved reduced lipid levels as well as decreased progression of atherosclerosis in mice (10). Furthermore, lowered levels of atherogenic lipoproteins in humans was also observed, and no serious adverse events were documented in the Phase I randomized clinical trial (10). These observations suggest that therapeutic antagonism of ANGPTL3 is effective and safe for reducing levels of lipids and incidences of atherosclerotic cardiovascular disease.

The microbial CRISPR-Cas9 system has been developed as a genome editing tool (11, 12). Cas9 introduces DNA double-strand breaks (DSBs) at sites targeted by a complementary guide RNA (gRNA). These DSBs are then repaired either by nonhomologous end joining or homology directed repair (13, 14). As compared with conventional ASO or antibody therapies, which are transient, the CRISPR-Cas9 system can induce permanent loss-of-function mutations, resulting in long-term therapeutic effects in the edited cells. However, the safe, efficient, and specific delivery of CRISPR-based therapies is a significant technical challenge, which has limited the therapeutic application of this technology. Viral vectors (such as adenovirus or adeno-associated virus) have been used for delivery of CRISPR-based therapies, including editing *Angptl3* (15), and while they can lead to high editing efficiency,

Significance

Genome editing technologies enable the permanent repair of disease-causing genetic mutations. However, the application of this technology has been limited by the technical challenge of achieving safe, effective, and specific in vivo delivery of the CRISPR-Cas9 genome editing components. Here, we report the development of a newly identified lipid nanoparticle (LNP) for specific delivery of CRISPR-Cas9 mRNA to the liver. While LNPs have been FDA approved for delivery of siRNA to the liver, here we examine their application for genome editing. When compared head-to-head, our delivery platform significantly outperforms the FDA-approved LNP in the efficient delivery of Cas9 mRNA for knockdown of the *Angptl3* gene and subsequent regulation of hypercholesterolemia, while matching the safety and specificity of the approved platform.

Author contributions: M.Q., Z.G., and Q.X. designed research; M.Q., Z.G., J.C., X.Z., X.R., Z.Y., and Y.L. performed research; M.Q., Z.G., M.H., X.J., F.Z., and Q.X. analyzed data; and M.Q., Z.G., F.Z., and Q.X. wrote the paper.

The authors declare no competing interest.

This article is a PNAS Direct Submission.

[1]M.Q. and Z.G. contributed equally to this work.

[2]To whom correspondence may be addressed. Email: qiaobing.xu@tufts.edu.

This article contains supporting information online at https://www.pnas.org/lookup/suppl/doi:10.1073/pnas.2020401118/-/DCSupplemental.

Published March 1, 2021.

they also carry significant safety risks associated with undesired insertional mutagenesis and potential biosafety (16, 17). An alternative, promising delivery modality is nonviral nanoparticles, such as lipid nanoparticles (LNPs), gold nanoparticles, or polymeric nanoparticles. LNPs have an advantageous safety profile and have been developed for the delivery of Cas9 plasmid DNA, mRNA, and ribonucleoproteins (RNPs), albeit with reduced delivery efficiency compared to viral vector approaches (18–20). We and others have previously reported using LNPs to successfully deliver CRISPR-Cas9 in both the RNP and mRNA formats (21–25). While delivering Cas9 as DNA, mRNA, or RNP (with gRNA) formats each have potential strengths, mRNA delivery is particularly promising for in vivo genome editing applications because of its transient, nonintegrating Cas9 expression feature.

Recently, LNPs have been explored by us and others for the delivery of Cas9 mRNA in vitro and in vivo. We recently demonstrated the use of bioreducible LNPs for the codelivery of Cas9 mRNA and gRNA, demonstrating highly efficient in vitro genome editing, as well as rapid knockdown of the *Pcsk9* cholesterol-regulating gene in vivo, highlighting the potential of this delivery approach (26). However, our previous study did not thoroughly examine the long-term therapeutic effects of this treatment. Recent research by Finn et al. (22) examined the ability to modulate the chemical structure of the Cas9 gRNA to influence the Cas9 editing efficiency in vivo to knock down the *Ttr* gene, a monogenic target overexpressed in certain orphan-designated amyloidosis diseases (22).

Here, we describe a highly potent nonviral LNP-mediated CRISPR-Cas9 delivery system for the liver delivery of Cas9 mRNA and demonstrate its efficacy by targeting the *Angptl3* gene. The system is composed of a leading tail-branched bioreducible lipidoid (306-O12B) coformulated with an optimized mixture of excipient lipid molecules, and it successfully codelivers SpCas9 mRNA and a single-guide RNA (sgRNA) targeting *Angptl3* (sgAngptl3) via a single administration (Fig. 1). 306-O12B LNP specifically delivered Cas9 mRNA and sgAngptl3 to liver hepatocytes of wild-type C57BL/6 mice, resulting in a median editing rate of 38.5% and a corresponding 65.2% reduction of serum ANGPTL3 protein. We found that delivery using 306-O12B LNP was more efficient than delivery with MC-3 LNP, a gold standard LNP that was recently approved by the US Food and Drug Administration (FDA) for liver-targeted delivery of nucleic acids (27). Moreover, liver specific knockdown of *Angptl3* resulted in profound lowering of LDL-C and TG levels. Importantly, no evidence of off-target mutagenesis at nine top-predicted sites was observed nor any apparent liver toxicity. The CRISPR-mediated genome editing was maintained at a therapeutically relevant level for at least 100 d after the injection of a single dose. The system we established here offers a clinically viable approach for liver-specific delivery of CRISPR-Cas9–based genome editing tools.

Results

In Vivo Screening of LNPs for mRNA Delivery. The tail-branched bioreducible lipidoids were prepared via a combinatory solvent free Michael addition reaction between disulfide bond-incorporated acrylate lipid tails and amine-containing heads according to our previous reports (Fig. 2*A*) (21, 28). We first evaluated the in vivo mRNA delivery efficacy of these lipids by encapsulating firefly luciferase mRNA (fLuc mRNA) into LNPs and delivering these LNPs intravenously to female wild-type Balb/c mice. These LNPs were formulated with our synthetic ionizable lipids, along with the excipient compounds cholesterol, DSPC, and DMG-PEG (polyethylene glycol). Representative transmission electron microscopy images of blank (unloaded) and fLuc mRNA-loaded LNPs are shown in *SI Appendix*, Fig. S1. The gold standard MC-3 LNP formulated with cholesterol, DSPC, and DMG-PEG was included as a positive control (29). Mice were injected intraperitoneally with luciferin substrate 6 h after mRNA delivery, and whole-body fLuc activity was measured using an in vivo imaging system (IVIS) (PerkinElmer). As shown in Fig. 2*B*, mRNA delivery with 306-O12B, 113-O12B, and 306-O10B LNPs resulted in comparable luciferase bioluminescence intensity as compared with MC-3 LNP delivery. In vivo images of mice showed that the luciferase protein was mainly expressed in the liver (*SI Appendix*, Fig. S2). Based on these preliminary results, we chose 306-O12B LNP for further development because of its relatively high luciferase expression as well as the high specificity. The fLuc mRNA could be efficiently encapsulated into the 306-O12B LNP with an encapsulation efficiency of ~96% (*SI Appendix*, Fig. S3). Following the encapsulation

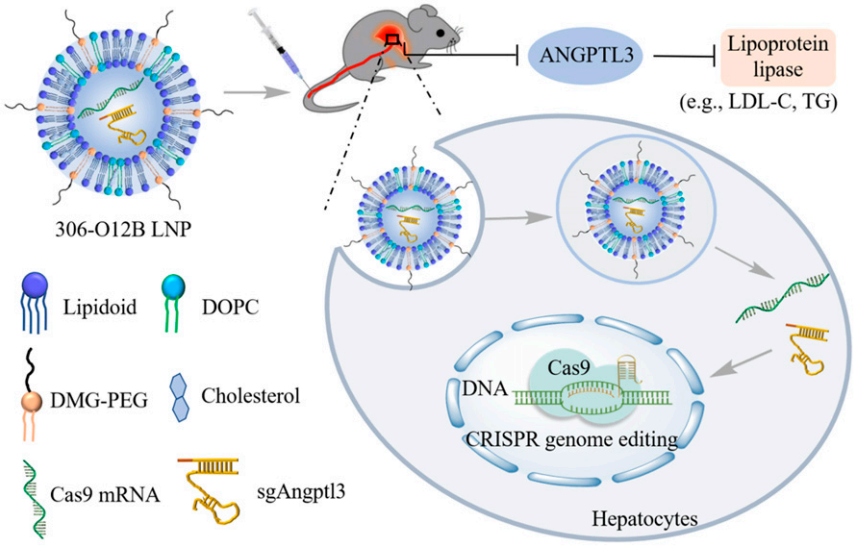

Fig. 1. Schematic illustration of LNP-mediated in vivo CRISPR-Cas9–based genome editing to induce loss-of-function mutations in *Angptl3* to lower blood lipid levels. The Cas9 mRNA and *Angptl3*-specific sgRNA (sgAngptl3) are encapsulated in the LNP and delivered to the liver hepatocytes where they cleave the *Angptl3* target locus, leading to reduced ANGPTL3 protein. Reduced ANGPTL3 level leads to a disinhibition of Lipoprotein lipase (LPL), which allows LPL to regulate the levels of therapeutically relevant circulating lipids such as LDL-C and TG.

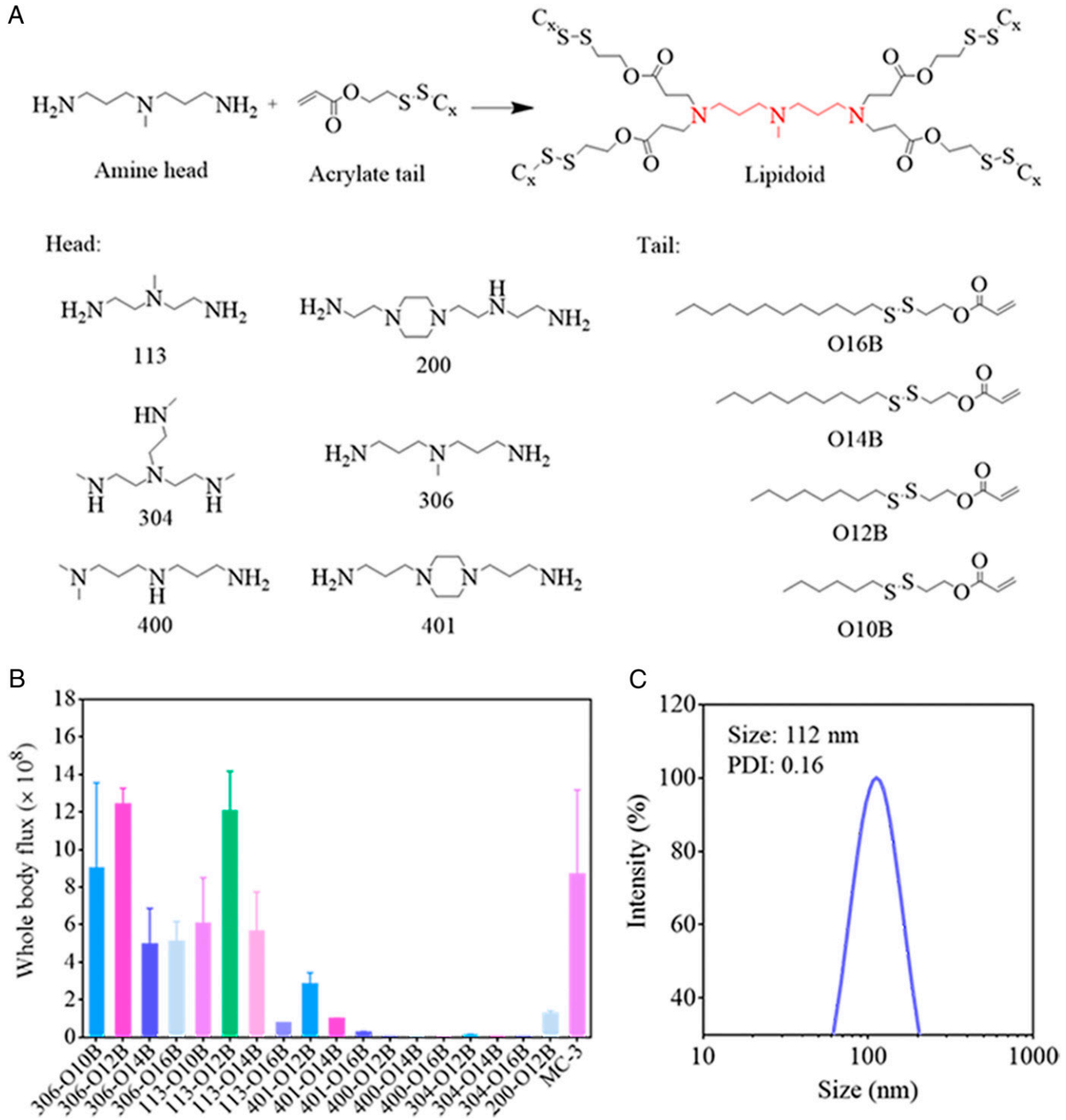

Fig. 2. Lipidoid nanoparticles synthesis. (*A*) Chemical structure of tail-branched bioreducible lipidoids. (*B*) Whole body luciferase bioluminescence intensity of bioreducible LNPs versus MC3 LNP measured in Balb/c mice (n = 3) at 6 h postadministration at an fLuc mRNA dose of 0.5 mg/kg. Formulation: lipid/cholesterol/DSPC/DMG-PEG = 50/38.5/10/1.5 (molar ratio), lipid/mRNA = 12.5/1 (weight ratio). (*C*) Size and distribution of 306-O12B LNPs formulated with fLuc mRNA measured by DLS.

of fLuc mRNA, 306-O12B LNP had an average diameter of 112 nm (Fig. 2*C*).

Optimization of the Formulation of 306-O12B LNP. To further increase the luciferase expression in vivo, we optimized a variety of formulation parameters used for the assembly of these LNPs, including the excipient phospholipid identity, the molar composition ratios of the four components of the LNP formulation, and the lipid/mRNA weight ratio of fLuc mRNA encapsulated 306-O12B LNP.

First, two additional phospholipids, DOPE and DOPC (Fig. 3*A*), which have similar structures but different head groups and tail saturation than the original DSPC phospholipid, were selected to evaluate the effect of phospholipid excipient on the efficacy of luciferase expression in vivo. DOPC and DOPE each contain one degree of unsaturation in the carbon tail, whereas

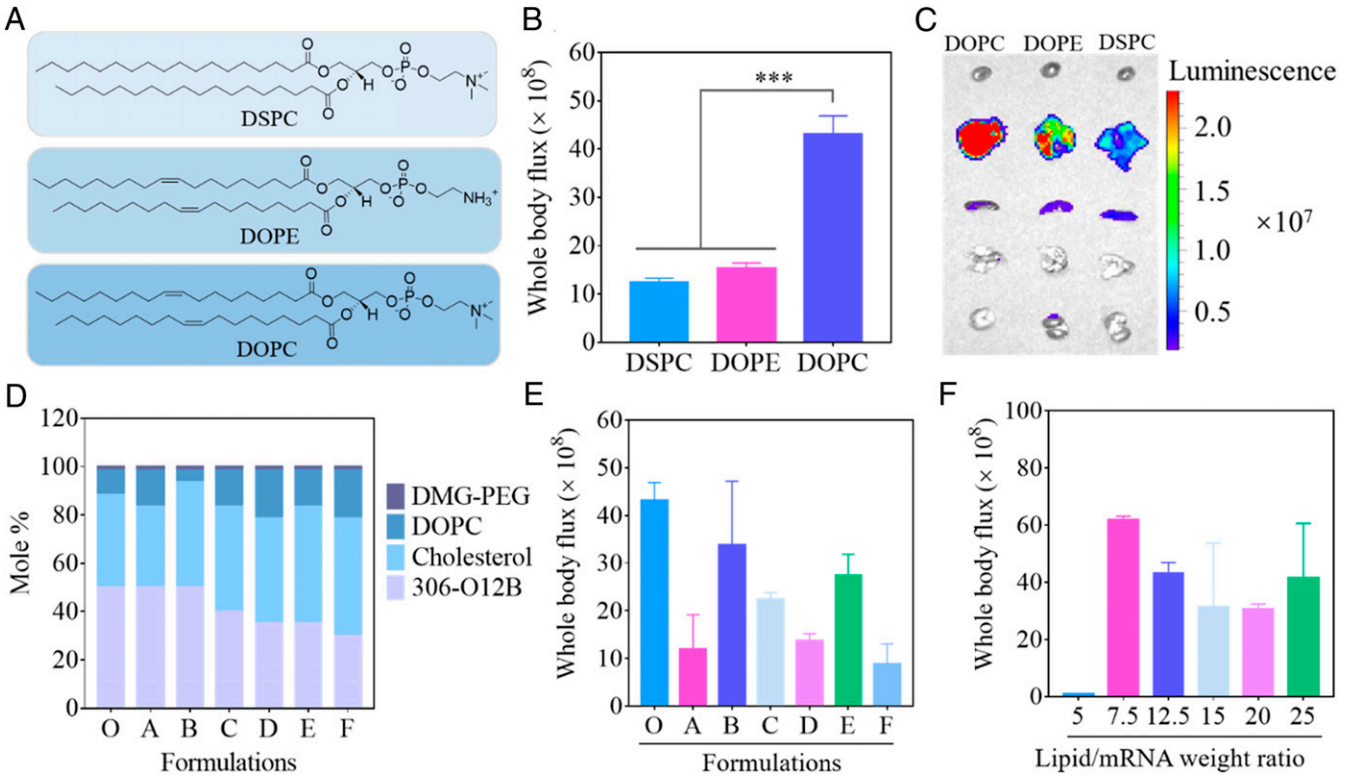

Fig. 3. Optimization of fLuc mRNA 306-O12B LNP formulations. (*A*) Chemical structure of three different phospholipids. Efficacy (*B*) and biodistribution (*C*) of fLuc mRNA LNPs formulated with Cholesterol, DMG-PEG, and different phospholipids (DSPC, DOPE, or DOPC). From top to bottom, luminescence signal is shown from the heart, liver, spleen, lungs, and kidneys of representative mice. $*P < 0.05$, $**P < 0.01$, $***P < 0.001$. (*D*) Formulation parameters of LNPs formulated with cholesterol, DOPC, and DMG-PEG at seven different mole ratios. (*E*) Whole body luciferase bioluminescence intensity of different formulations in Balb/c mice at 6 h postinjection at a fLuc mRNA dose of 0.5 mg/kg. (*F*) Whole body luciferase bioluminescence intensity 6 h postinjection of 0.5 mg/kg fLuc mRNA for LNPs formulated with cholesterol, DOPC, and DMG-PEG at a molar ratio of 50/38.5/10/1.5 with differing 306-O12B/mRNA weight ratios ($n = 3$).

DSPC is fully saturated. Furthermore, DSPC and DOPC each contain a quaternary amine headgroup, whereas DOPE contains a primary amine headgroup. Each of these features has been reported to influence LNP delivery efficiency in the literature (30). It has been reported that quaternized amine headgroups show a stronger proton sponge effect than primary amine headgroups (31), which can facilitate the endosomal escape of the cargo mRNA into the cytoplasm, thus increasing translation of the mRNA. Furthermore, the degree of saturation of the lipid tail has been shown to influence membrane fluidity, which may also influence endosomal escape. Unsaturated lipid tails may result in higher membrane fluidity, which may also help improve endosomal escape via destabilization of the endosomal membrane upon fusion of the LNP with the membrane (30, 32). Based on these reports, we hypothesized that LNPs formed with DOPC, which contains a quaternary amine and unsaturated tail, would show the most efficient fLuc delivery. As shown in Fig. 3 *B* and *C*, fLuc mRNA LNPs formulated with DOPC indeed resulted in significantly higher luciferase expression in the liver than that of formulations with DOPE and the original DSPC phospholipid. fLuc mRNA delivered with DOPC-containing LNPs resulted in ~fourfold higher luminescence signal compared to the original DSPC-containing LNPs.

In our initial screenings, the active lipid and excipient components were formulated at a molar ratio of [Lipid:Cholesterol:DSPC:DMG-PEG] of [50:38.5:10:1.5]. This excipient ratio has been reported in the literature to be effective (29). After identifying the optimal phospholipid as DOPC and adjusting the formulation accordingly, we tested LNPs formulated at a variety of molar ratios to identify the optimal parameters (Fig. 3*D*). As shown in Fig. 3*E*, the original formulation O (306-O12B:cholesterol:DOPC:DMG-PEG at a molar ratio of 50:38.5:10:1.5) displayed the highest luciferase bioluminenscence intensity; none of the new formulation parameters surpassed the original.

In an effort to further increase the in vivo efficacy, the LNPs with this optimal ratio of four components were formulated with different weight ratios of active lipid 306-O12B: mRNA ranging from 5:1 to 25:1. Interestingly, we found that the highest efficacy was achieved when the weight ratio was 7.5:1. It appears as though increasing the amount of lipid beyond this point does not improve in vivo delivery efficacy (Fig. 3*F*). Collectively, these results indicated that the optimized formulation of 306-O12B LNP had 50% 306-O12B, 38.5% cholesterol, 10% DOPC, and 1.5% DMG-PEG molar composition with a 7.5:1 weight ratio of 306-O12B/mRNA.

In Vivo Hepatocyte-Specific Codelivery of Cas9 mRNA and sgRNA with mRNA-Optimized 306-O12B LNP. Identification of the specific cell types that are preferentially edited by Cas9 mRNA/sgRNA LNPs is critical for evaluating the potential applications of a CRISPR delivery system. We used the Ai14 reporter mouse line, which is genetically engineered with a LoxP-Flanked STOP cassette controlling tdTomato expression (33). Although this mouse line is frequently used with Cre recombinase, successful CRISPR-mediated excision of the LoxP-flanked stop codon will also induce the expression of tdTomato (34). When paired with Cas9 and a gRNA targeting this site, examination of the cells with tdTomato expression indicates which cell types our LNP delivery system targets.

To validate this approach, we first used the 306-O12B LNP to deliver the LoxP-targeted sgRNA (sgLoxP) to mice engineered to express both the Ai14 construct and a constitutively expressed Cas9 construct (Ai14+/Cas9+ mouse model) (35). As shown in *SI Appendix*, Fig. S4, delivery of sgLoxP with our optimized

306-O12B LNP system resulted in red fluorescence detected specifically in the liver. Interestingly, further histological analysis revealed that the tdTomato signal was mainly observed in the liver hepatocytes, indicating that 306-O12B LNP can also specifically deliver sgRNA to this therapeutically relevant cell type.

Next, Cas9 mRNA and sgLoxP were coformulated into one single LNP and injected into Ai14 mice via tail vein at 1.65 mg/kg total RNA dose (*SI Appendix*, Fig. S5*A*). Organs were harvested 7 d after delivery and imaged ex vivo using the IVIS system. Imaging of mouse organs showed that this system could indeed induce red fluorescence, indicating successful functional codelivery of both the mRNA and sgRNA components, and that tdTomato signal was predominantly detected in the liver (*SI Appendix*, Fig. S5*B*). Immunofluorescent staining for hepatocyte specific antigen was also performed, and the confocal images demonstrated that the majority of the tdTomato protein was expressed in the hepatocytes (*SI Appendix*, Fig. S5*C*). These findings indicate that 306-O12B LNP can specifically transport Cas9 mRNA and gRNA to liver hepatocytes.

In Vivo Genome Editing of *Angptl3*. Encouraged by the positive results achieved above, we next tested the ability of 306-O12B LNP to deliver Cas9 mRNA to manipulate the expression of a functional endogenous gene, *Angptl3*. *Angptl3* encodes angiopoietin-like 3 (ANGPTL3), a central regulator of lipoprotein metabolism which inhibits both lipoprotein lipase and endothelial lipase activity (3). We first explored the ratio of Cas9 and gRNA, which may affect the in vivo genome editing efficacy, by injecting C57BL/6 mice with 306-O12B LNP coformulated with different Cas9 mRNA to sgAngptl3 mass ratios of 2:1, 1:1.2, and 1:2 at a total RNA dose of 3.0 mg/kg. Nanoparticles were formulated using the optimized formulation parameters determined above; namely, helper molecules at a molar ratio of 50:38.5:10:1.5 (306-O12B:cholesterol:DOPC:DMG-PEG), with a 306-O12B to total RNA weight ratio of 7.5:1. At day seven after injection, blood serum was collected for enzyme-linked immunosorbent assay (ELISA) analysis of serum ANGPTL3 protein levels, and liver tissue samples were collected for DNA extraction and next-generation sequencing (NGS) to determine targeted Cas9-mediated genome editing. We observed genome editing in liver tissue and a reduction of serum ANGPTL3 protein levels at all Cas9 mRNA/sgAngptl3 ratios; however, no significant differences were observed between these groups (Fig. 4). A ratio of 1:1.2 Cas9 mRNA/sgAngptl3 was used for the following experiments. The Cas9 mRNA/sgAngptl3 encapsulated 306-O12B LNP had similar characteristics as fLuc mRNA LNP with an average size of 110 nm (*SI Appendix*, Fig. S6).

Given the significant levels of editing, we next designed and performed a more detailed in vivo editing experiment. As a gold standard, we compared our 306-O12B LNP against LNP composed of the FDA-approved liver-targeting lipid MC-3 (termed MC3 LNP), encapsulating the same RNA components. Mice were administered with 306-O12B LNP or MC-3 LNP at a total RNA dose of 3.0 mg/kg. At day seven after administration, we observed the editing at the desired site in the liver using a T7E1 assay (*SI Appendix*, Fig. S7). NGS of the *Angptl3* target site in liver samples further demonstrated that 306-O12B LNP-mediated delivery resulted in a median editing rate of 38.5%, which is significantly higher than that of MC-3 LNP mediated delivery (14.6%) (Fig. 5*A*). More importantly, the serum analyses revealed that the serum ANGPTL3 protein, LDL-C, and TG levels in 306-O12B LNP treatment group (65.2, 56.8, and 29.4% reductions, respectively) were significantly lower than that of MC-3 LNP treated mice (25, 15.7, and 16.3% reductions, respectively) (Fig. 5*A*). A detailed analysis of the NGS sequencing results revealed that the most frequent editing event was a 1-nt deletion precisely at the predicted Cas9 cut site, followed by a 1-nt insertion at the same location (Fig. 5*B*). As expected, the same editing events were observed in both MC3 LNP and 306-O12B LNP-treated livers; the main difference was in the frequency of these events. This indicates that the observed serum component reductions were likely a result of the Cas9-mediated genome editing and implies that the difference in observed outcomes between the two lipids was solely a result of delivery efficiency, rather than a change in the innate activity of the Cas9 mRNA.

With any CRISPR delivery system, care must be taken to avoid off-target editing events or delivery-induced toxicity. The top nine most likely off-target genomic mutagenesis sites were predicted computationally, and these loci were interrogated via NGS of DNA extracted from the liver. No evidence of editing at any of the nine top-predicted off-target mutagenesis sites was observed (Fig. 5*C*). To evaluate the in vivo toxicity and potential immunoinflammatory response, serum levels of the liver function markers aspartate aminotransferase (AST), alanine aminotransferase (ALT), and of the proinflammatory cytokine tumor necrosis factor-alpha (TNF-alpha) were measured 48 h postdose. No significant changes in these markers were detected after treatment with the Cas9 LNP (*SI Appendix*, Fig. S8). In addition, we further observed that the serum cytokine levels, i.e., IFN-α, IL-6, and IP-10 were up-regulated at 6 h postadministration. However, by 48 h postadministration, the level of all cytokines returned to baseline, indicating that the delivery does not induce a long-term systemic inflammatory response (*SI Appendix*, Fig. S9).

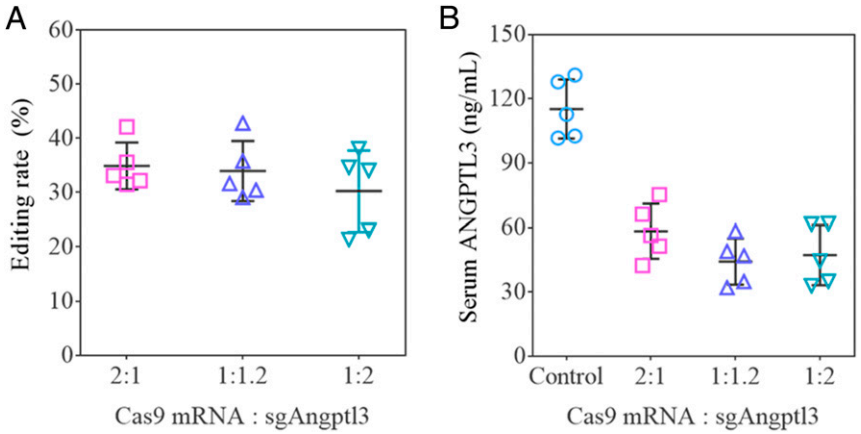

Fig. 4. 306-O12B LNP-mediated significant levels of in vivo genome editing of *Angptl3* in wild-type C57BL/6 mice. Indels percentage (*A*) and serum ANGPTL3 levels (*B*) following injections of 306-O12B LNP formulated with Cas9 mRNA and sgAngptl3 at a mass ratio of 2:1, 1:1.2, and 1:2 ($n = 5$). 306-O12B LNP was formulated at a molar ratio of [306-O12B:Cholesterol:DSPC:DMG-PEG] of [50:38.5:10:1.5] with a 7.5/1 weight ratio of 306-O12B/total RNAs.

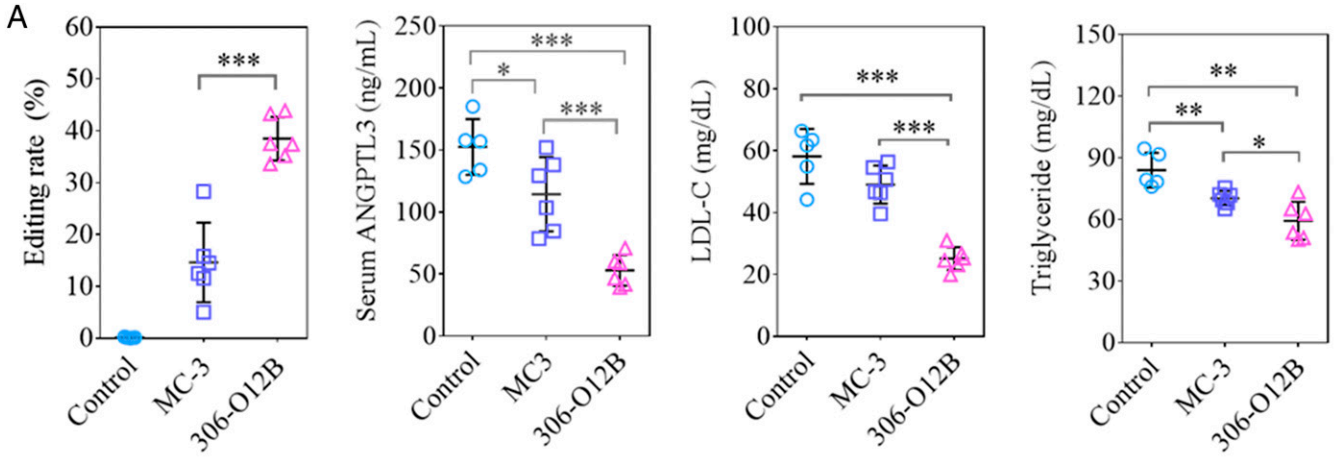

B

Edited ANGPTL3 sequence	Mutation type	frequency in 306-O12B (%)	frequency in MC-3 (%)	frequency in control (%)
CGTTTTTAACTTGTAGTGTA	wild-type			
CGTTTT_AACTTGTAGTGTA	1nt deletion	24.6	9.1	0.1
CGTTTTT|AACTTGTAGTGTA T	1nt insertion	10.3	4.5	0.0
CGTTT__AACTTGTAGTGTA	2nt deletion	1.3	0.4	0.0
other edits		2.5	0.7	0.1
total edited alleles		38.7	14.7	0.2

C

Potential off-target site	Location	frequency in 306-O12B (%)	frequency in MC-3 (%)	frequency in control (%)
aACACTACAA-TTAAAAACGTGG	chr17: 67139471	0.06	0.03	0.06
TACACTAaAA-TTAAAAACGTGG	chr10: 96372376	0.01	0.04	0.06
TtCACTACAAGTTAGAAAACaGGG	chr3: 96010269	0.04	0.03	0.03
TACACTACGAAaTTAAAAcCGAGG	chr14: 113652925	0.04	0.03	0.02
TACACTACAAGTTCAAAtACaTGG	chr9: 20240345	0.02	0.02	0.02
TACACTA-AAGaTAAAAACaTGG	chr8: 57778609	0.04	0.04	0.04
TACAgT-CAAGTTAAAAACcAGG	chr12: 53110237	0.07	0.10	0.07
T-CACTACtAGaTAAAAACGTGG	chr3: 65249939	0.04	0.04	0.03
cACACTACAAG-TAAAAACaGGG	chr3: 38440103	0.04	0.05	0.04

Fig. 5. 306-O12B LNP is more efficient than MC-3 LNP in inducing loss-of-function mutations in *Angptl3* through CRISPR-Cas9–based genome editing. (*A*) NGS analysis of the indels in liver and serum analyses of ANGPTL3 protein, TG, and LDL-C level of mice at day seven postadministrated with Cas9 mRNA and sgAngptl3 coloaded 306-O12B LNP at a total RNA dose of 3.0 mg/kg. MC-3 LNP was used as a positive control ($n = 5$ or 6). *$P < 0.05$, **$P < 0.01$, ***$P < 0.001$. (*B*) Editing frequencies of specific edited alleles in each treatment group. (*C*) Editing frequencies at nine top predicted off-target sites.

One of the tremendous advantages of CRISPR-Cas9 over other therapies is the potential to generate a long-term therapeutic efficacy with only one injection. To assess the long-term durability of editing and knockdown in the liver, we injected 306-O12B LNP into C57BL/6 mice at a total RNA dose of 1.0, 2.0, or 3.0 mg/kg. Importantly, we found that the therapeutic effect was stable for at least 100 d after a single dose administration. A dose-dependent genome editing of *Angptl3* in the liver and knockdown of serum ANGPTL3 was still observed 100 d after a single administration, with profound reductions in serum ANGPTL3, LDL-C, and TG levels (60, 48.1, and 28.6% reductions, respectively) at the highest dose (Fig. 6*A*). This indicates both the potential ability to titrate the knockdown effect by varying the total RNA dose, and the ability of a single dose to generate a therapeutically relevant knockdown effect over a longer time scale. No evidence of long-term systemic toxicity was observed (Fig. 6*B*). Furthermore, continued observation has indicated that the genomic editing could still be detected at least 150 d after the single, initial administration of 306-O12B LNP (*SI Appendix*, Fig. S10). While further study is necessary to establish the maximum duration of genomic editing effects after a single administration, as well as to confirm that the serum lipid profile continues to track with the

genomic editing profile over longer time periods; this is a promising indicator of the long-term efficacy of our delivery platform.

Taken together, these results indicated that our 306-O12B LNP is more efficient than the gold standard MC-3 LNP in inducing loss-of-function mutations in *Angptl3* through CRISPR-Cas9–based genome editing. The nonviral LNP mediated in vivo genome editing of *Angptl3* in the liver led to therapeutically relevant reduction of blood lipid levels (8, 10), with minimal off-target editing events, systemic toxicity, or inflammation in the mouse.

Discussion

We show here a highly potent lipidoid nanoparticle, composed of the synthetic, bioreducible lipidoid 306-O12B, capable of liver specific delivery of Cas9 mRNA and gRNA for in vivo *Angptl3* editing. In recent years, the CRISPR-Cas9 system has emerged as a potent therapeutic platform to correct genetic disorders for disease treatment. However, the application of this technology has been significantly hampered for a number of reasons, many relating to the lack of safe and efficient delivery vehicles. First, the large size of the Cas9-gRNA complex makes it difficult to encode the entire complex within a single viral genome or to deliver the 160 kDa protein directly into cells. Second, the host immune response to the CRISPR machinery or the delivery vector itself, as well as preexisting anti-Cas9 antibodies or anti–adeno-associated virus (AAV) antibodies in humans, can result in dramatically reduced CRISPR efficacy and potential immunotoxicity. Finally, the potential undesired host genome insertional mutagenesis of the CRISPR construct, or off-target genomic editing events caused by insufficient specificity of the CRISPR machinery, may induce fatal genotoxicity (36). Some of these issues can be ameliorated by delivering Cas9 as mRNA in complex with gRNA. For example, unlike plasmid DNA or virus, mRNA does not need to be transported into the cell nucleus; the translation of mRNA to protein occurs in the cytoplasm, thus simplifying the delivery path and avoiding the possibility of insertional mutagenesis of the CRISPR machinery (37). Furthermore, delivery of an mRNA compound results in transient expression of the CRISPR components, unlike viral delivery which may result in prolonged expression. It has been suggested that transient expression may reduce off-target genomic editing simply by reducing the opportunity for such adverse editing events to occur (38).

To facilitate the clinical translation of mRNA-mediated CRISPR technology, delivery systems with superb safety, high specificity, and efficacy are needed. Nonviral nanoparticles prepared from synthetic biomaterials have shown promise to improve cytosolic delivery of nucleic acids in vivo. LNPs are one of the most developed formulations for RNA delivery. In August 2018, the U.S. FDA approved the first LNP-based siRNA formulation (27). Encouraged by the success of LNPs, tremendous efforts have been made using LNPs for in vivo mRNA transfection (39–41).

In vitro potency of an LNP formulation, however, rarely reflects its in vivo performance, and we therefore directly conducted in vivo screening of a library of tail-branched bioreducible lipidiods in our study. We found that the amine heads and the hydrophobic chain length in the lipidoids play critical roles in

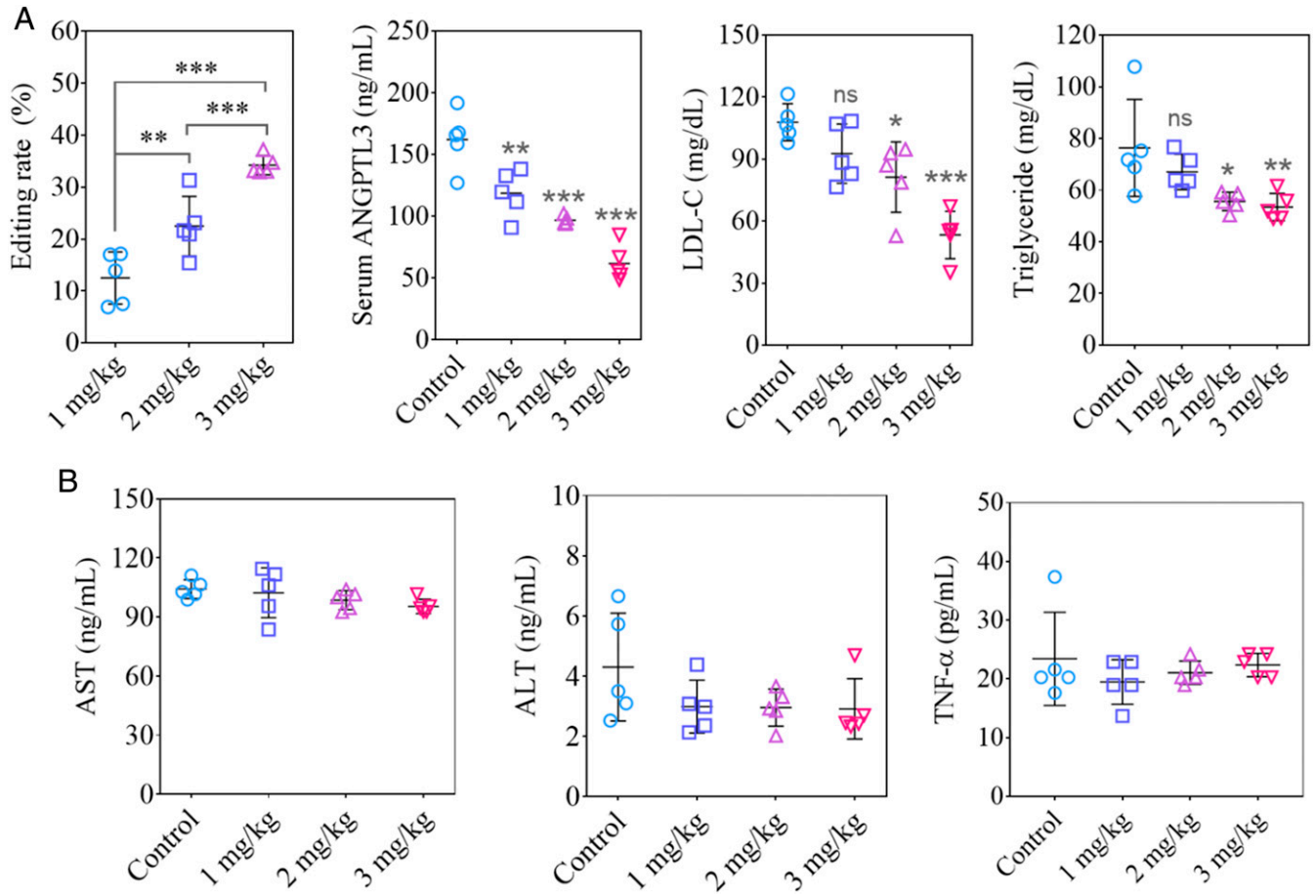

Fig. 6. 306-O12B LNP-mediated CRISPR editing remains durable after 100 d. (*A*) NGS analysis of the indels in liver and serum analyses of ANGPTL3 protein, TG, and LDL-C level of mice at day 100 postadministrated with Cas9 mRNA and sgAngptl3 coloaded 306-O12B LNP. (*B*) Serum levels of AST and ALT and TNF-alpha measured at day 100 postinjection. Female C57BL/6 mice were systemically injected with 306-O12B LNP coformulated with Cas9 mRNA and sgAngptl3 with a single dose at 1.0, 2.0, and 3.0 mg/kg of total RNA. Mice serum were collected at day 100 after injection ($n = 5$). *$P < 0.05$, **$P < 0.01$, ***$P < 0.001$.

determining in vivo mRNA delivery efficacy. Lipid nanoparticle formulations are typically composed of an ionizable active lipid, a phosphor helper lipid, cholesterol, and lipid-anchored PEG. The relative ratio of these components may have profound effects on the in vivo mRNA delivery efficacy. We used the published formulation conditions of MC-3 LNP as a starting formulation for our study. While the structure of our lipidoid is different from MC-3, our previously published LNPs use similar excipient lipids as those used for MC-3 LNP. We hypothesized that the excipient lipid components may serve a similar role in both types of LNPs and thus using similar excipient ratios would provide a valid starting point. To further maximize protein expression in vivo, we experimentally optimized these formulation parameters for our LNP. We found that the optimal formulation for our LNP contained 50% 306-O12B, 38.5% cholesterol, 10% DOPC, and 1.5% DMG-PEG (by molar ratio) with a 7.5:1 weight ratio of 306-O12B to mRNA.

Previous reports have shown that inhibition of ANGPTL3 activity by ANGPTL3 antibody or ASO provided therapeutically beneficial reduction in TG and LDL cholesterol levels in humans (8, 10). Further, the complete loss of function of *Angptl3*, which has been found naturally occurring in certain families, does not appear to cause adverse health consequences in humans. *Angptl3* is predominantly expressed in the liver, an ideal target organ for in vivo genome editing because of its tissue accessibility by intravenous injection. Together, these features make *Angptl3* an attractive therapeutic target for genome editing. In this work, we observed that the genome editing enabled by delivery of Cas9 mRNA and gRNA with our 306-O12B LNP occurs mainly in hepatocytes, as determined by the biodistribution of fluorescent signal in the Ai14 model mouse line. Moreover, we observed that the serum TGs and LDL-C levels are effectively reduced as a result of the hepatocyte-specific disruption of *Angptl3*.

The 306-O12B LNP led to more efficient genome editing than MC-3 LNP at the same dose of mRNA. Notably, a recent preclinical study of ASO-mediated silencing of *Angptl3* in a similar mouse model achieved a 50% reduction in serum ANGPTL3 protein levels, 7% reduction of LDL-C, and 35% reduction in TG levels (10). A single dose of our CRISPR-mediated knockdown using 306-O12B LNP matched or exceeded these knockdown benchmarks (65.2, 56.8, and 29.4% reductions, respectively), while MC3 LNP did not (25, 15.7, and 16.3% reductions, respectively). That particular ASO mouse study was followed up with a Phase I human clinical trial, suggesting the levels of knockdown we achieved are likely therapeutically relevant. Direct comparisons of our mouse study to human clinical trials for ANGPTL3 antibody or ASO therapies, however, are challenging because of the differences in species and dosing regimens. Clinical trials of both ASO and antibody therapies have demonstrated the ability to titer the percentage knockdown of these factors based on dosage amount and frequency and in particular saw the strongest effects upon multiple repeated doses of drug per patient at the highest experimental dose level. While a thorough clinical dosage analysis falls beyond the scope of this study, we did observe a dose-dependent reduction in serum ANGPTL3 levels upon a single injection of 306-O12B LNP. This indicates to us that in a clinical setting, our LNP system could achieve similar dose- and frequency-dependent knockdown, and that under the correct dosage scheme we could achieve a similar magnitude of knockdown as reported in these clinical trials. Importantly, we reported that the knockdown effects of a single dose, detectable at the genomic and protein levels, as well as in the downstream therapeutic metrics, were stable for at least 100 d. The human clinical trials indicated a maximum knockdown effect within 1 wk of receiving the drug, with serum levels slowly returning to baseline over the subsequent months. While this result is expected, as CRISPR generates a permanent change in the target cell's genome, while ASOs and antibodies are transient treatments, this difference is particularly notable and may have tremendous therapeutic consequences.

It has been reported that in vivo CRISPR mRNA delivery may result in a genomic knockdown which is durable for at least one full year after administration (22). Although our thorough analysis of serum lipid levels was only performed out to 100 d after administration, sequencing data indicated durable genomic editing at least to 150 d. Our data indicates a very slight reduction in genomic editing efficiency over time, which may reflect the slow turnover of hepatocytes in the liver, which have a predicted life of ~300 d (42). Regardless, our data are not incompatible with the possibility of therapeutic efficacy out to 1 y. Notably, we report that the genomic editing efficiency of a 3 mg/kg dose detected at 150 d after injection (31%) is still higher than the editing efficiency of a lower 2 mg/kg dose detected at only 100 d after injection (22%). The 22% genome editing rate was sufficient to generate a statistically significant reduction of ANGPTL3 protein, as well as serum cholesterol and LDL-C. Thus, it is highly likely that the full suite of therapeutic metrics would also show a significant knockdown out to 5 mo or beyond. This point warrants further study.

In addition to genome editing efficacy, off-target effects are a major concern for the clinical translation of CRISPR-Cas9 technology. Off-target effects can be discussed in two contexts: off-target delivery effects (i.e., the delivery of a liver drug to the kidneys) and biological off-target editing (i.e., editing events at unintended genomic loci). In this work, we used the luciferase and tdTomato model systems to demonstrate specific delivery to the liver and specifically hepatocytes, largely minimizing off-target delivery effects. To address the biological off-target editing issue, we designed a highly specific sgRNA target to *Angptl3* by using publicly available computational-based design tools to mitigate off-target editing events. Targeted NGS data confirmed that no editing was detected in the liver at the top nine off-target sites predicted by Cas-Off-Finder. While further studies using techniques such as whole-genome sequencing and direct comparisons to viral-mediated CRISPR delivery or other guide sequences may be necessary to further validate the safety of our platform for general liver delivery applications, the data presented here suggests that under the conditions examined, 306-O12B LNP were found to be highly specific with regards to both off-target delivery and off-target editing. From a systemic perspective, our LNP system did not cause any significant changes to ALT or AST levels, markers of liver health, and our data indicates that our LNP are not detectably toxic to the liver. Similarly, the lack of significant change in TNF-alpha indicates that our LNPs delivery does not induce a significant immune response. Together, this indicates that our treatment is safe in mice.

Outcomes of this study may advance the systemic delivery of CRISPR genome editing machinery in the clinic. To realize the final clinical application, more detailed preclinical studies for the chronic tolerability, off-target effects, and the efficacy in large animals should be performed in the future. Overall, we demonstrate here that 306-O12B LNP is a highly potent and safe nonviral delivery platform for clinically relevant liver-specific CRISPR-Cas9–based genome editing.

Materials and Methods

Study Design. The overall objective of this study is to explore a nonviral LNP-mediated CRISPR-Cas9 mRNA-based strategy for in vivo organ-specific genome editing of *Angptl3* for blood lipids regulation. We addressed this objective by 1) identifying a liver-targeted bioreducible lipid nanoparticle platform that can effectively deliver mRNA to hepatocytes; 2) optimizing the LNP formulation to maximize the in vivo mRNA delivery efficacy; 3) demonstrating in vivo genome editing effects of 306-O12B LNP-mediated Cas9 mRNA delivery by targeting the therapeutically relevant *Angptl3* gene, resulting in profound reductions in serum ANGPTL3, LDL-C, and TG levels; and 4) revealing that the therapeutic effect of LNP-mediated CRISPR-Cas9 mRNA-based genome editing of *Angptl3* was stable for at least 100 d after a single dose administration. All animal experiments were conducted according to the protocols approved by the Tufts University Institutional Animal Care and Use Committee (IACUC) and performed in accordance with the NIH guidelines for the care and use of

experimental animals. The genome editing efficacy, off-target side effects, safety profile, and changes in levels of lipids were thoroughly evaluated.

LNPs Formulation. The lipidoids were synthesized as per our previous reports (21, 28). LNPs were prepared using a NanoAssemblr microfluidic system (Precision Nanosystems). Briefly, lipidoids, cholesterol (Sigma), phospholipids (DSPC, DOPE, and DOPC, Avanti Polar Lipids), and methoxypolyethylene glycol (DMG-PEG_{2000}) (Avanti Polar Lipids) were dissolved in 100% ethanol at molar ratios of 50/38.5/10/1.5 at a final lipidoids concentration of 10 mg/mL. The MC-3 LNP formulation was prepared by following the procedure as previously described by Sedic et al. (29) with a slight modification. In brief, the lipids (6Z,9Z,28Z,31Z)- heptatriaconta-6,9,28,31-tetraen-19-yi 4-(dimethylamino)butanoate (MC-3), DSPC, Cholesterol, and DMG-PEG_{2000} were dissolved in pure ethanol at a molar ratio of 50% MC-3, 38.5% Cholesterol, 10% DSPC, and 1.5% DMG-PEG_{2000} with a final MC-3 concentration of 10 mg/mL. The lipid solution was then mixed with an acidic sodium acetate buffer containing mRNA (0.45 mg/mL, pH 4.0) by using the NanoAssemblr microfluidic system. The resulting LNP was dialyzed against phosphate-buffered saline (PBS) (pH 7.4, 10 mM) overnight at 4 °C. Cas9 mRNA and gRNA (either sgANGPTL3 or sgLoxP) were mixed at the appropriate weight ratio in sodium acetate buffer (25 mM, pH 5.2). The mRNA solution and the lipid solution were each injected into the NanoAssemblr microfluidic device at a ratio of 3:1, and the device resulted in the rapid mixing of the two components and thus the self-assembly of LNPs. Formulations were further dialyzed against PBS (10 mM, pH 7.4) in dialysis cassettes overnight at 4 °C. The particle size of formulations was measured by dynamic light scattering (DLS) using a ZetaPALS DLS machine (Brookhaven Instruments). RNA encapsulation efficiency was characterized by Ribogreen assay.

In Vivo LNPs Delivery. All procedures for animal experiment were approved by the Tufts University IACUC and performed in accordance with the NIH guidelines for the care and use of experimental animals. All the animals were ordered from Charles River. Female Balb/c mice (6 to 8 wk) were used for in vivo fLuc mRNA (TriLink Biotechnologies) encapsulated LNPs screening and formulations optimization. Briefly, fLuc mRNA LNPs were intravenously injected into the mice at a dose of 0.5 mg/kg mRNA. At a predetermined time point, mice were injected with 100 μL D-Luciferin potassium salt (Goldbio) solution (15 mg/mL in PBS), anesthetized under isoflurane anesthesia, and measured by IVIS imaging system (Caliper Life Sciences).

Commercially Sourced Nucleic Acids. Cas9 mRNA was sourced from Tri-Link Biotechnologies. All sgRNAs used in this manuscript were sourced from Synthego using their "end-modified" synthesis. Briefly, the first and last three bases of these gRNA were synthesized using 2′-O-Methyl-nucleosides and joined via 3′ phosphorothioate bonds. All other bases throughout the rest of the molecule are traditional ribonucleosides and phosphate bonds that are typical for native RNA.

In Vivo Cas9 mRNA/sgLoxP Delivery. Cas9 mRNA (TriLink Biotechnologies) and LoxP-targeted sgRNA (sgLoxP, sequence: 5′-AAGTAAAACCTCTACAAATG, end modified, Synthego) were coloaded into 306-O12B LNPs and intravenously injected into female Ai14 mice at a dose of 1.65 mg/kg total RNA. At day seven postinjection, mouse organs were collected and imaged by IVIS to detect the tdTomato expression. The liver tissue was further sectioned.

Immunostaining. Tissue samples were embedded in optimal cutting temperature (OCT) compound, frozen completely in liquid nitrogen, and stored at –80 °C until ready for sectioning. The frozen tissue block was sectioned into a desired thickness (10 μm) using the cryotome and placed onto glass slides suitable for immunofluorescence staining. The tissue sections were fixed with precooled acetone (–20 °C) for 10 min and then washed twice with PBS for 5 min each. The fixed tissue sections were incubated in 10% bovine serum albumin (BSA) blocking buffer at room temperature (r.t.) for 1 h and then washed with PBS. A hepatocyte specific primary antibody (1:100 diluted in 1% BSA buffer, anti-hepatocyte specific antigen [HepPar1], Novus) (43) was applied to the sections on the slides and incubated in a humidified chamber at 4 °C overnight. The slices were rinsed with PBS for two changes for 5 min each and then stained with eFlour660 conjugated F(ab')2-Goat anti-mouse secondary antibody (1:50, Invitrogen) and incubated in a humidified chamber protected from light at r.t. for 1 h and then washed three times with PBS. Fluorescent mounting medium containing 4′,6-diamidino-2-phenylindole (DAPI) (Sigma) was used to coverslip the slides. Sections were analyzed using a Leica SP8 confocal microscope.

In Vivo Genome Editing of *Angptl3*. gRNA sequence targeting *Angptl3* was designed using the Benchling software. Female wild-type C57BL/6 mice, aged 6 to 8 wk, were intravenously dosed with Cas9 mRNA and ANGPTL3-targeted sgRNA (sgAngptl3, sequence: 5′-AGCCCTTCAACACAAGGTCA, end modified, Synthego) coloaded 306-O12B LNP at a dose of 1.0, 2.0, and 3.0 mg/kg in total RNA. PBS administrated mice were treated as negative control. At day seven postinjection, mice were euthanized (without fasting), blood was collected for circulating ANGPTL3 protein and blood lipids quantitation by ELISA, and liver tissue was collected from the median and left lateral lobe for DNA extraction and NGS analysis. To control for the influence of circadian rhythm on serum lipid levels, serum was collected at approximately the same time of day (early afternoon) for all experiments. In addition, to evaluate the in vivo toxicity and immune response, blood was collected and proceeded to serum from mice 2 d after the injection. AST, ALT, and TNF-alpha were measured using assay kits for AST (G-Biosciences), ALT (G-Biosciences), and TNF-alpha (R&D Systems) per manufacturer's protocols. Serum levels of IFN-α, IL-6, and IP-10 were determined with the mouse IFN-α ELISA Kit (PBL Assay Science), mouse IL-6 Quantikine ELISA Kit (R&D Systems), and Abcam mouse IP-10 ELISA Kit, respectively.

NGS Sequencing Analysis. DNA was extracted from the median and left lateral lobe of the liver using a commercial extraction kit (Qiagen DNEasy Blood and Tissue). PCR primers were designed to amplify the region surrounding the target site in the Angptl3 gene or the regions surrounding the predicted off-target sites (*SI Appendix*, Table S1). Off-target sites were predicted using the Cas-Off-Finder software (www.rgenome.net/cas-offinder/http://rgenome.net/cas-offinder/) (44). PCR amplicons were prepared for sequencing on an Illumina MiSeq (Tufts Genomics Core Facility). Sequencing data were analyzed using the OutKnocker 2 software (www.outknocker.org/outknocker2.htm) (45).

Serum ANGPTL3 Protein, LDL-C, and TG Analysis. Mouse blood was collected without using an anticoagulant and was allowed to clot for 2 h at r.t. and centrifuged at 2,000 × g for 15 to 20 min at r.t. to collect mouse serum. Serum levels of ANGPTL3 protein, LDL-C, and TG were determined using a Mouse Angiopoietin-like 3 Quantikine ELISA kit (R&D systems), Mouse LDL-Cholesterol kit (Crystal Chem), and TG Colorimetric Assay kit (Cayman Chemical) as per manufacturer's protocols, respectively.

T7E1 Cleavage Assay. The genomic regions flanking the on-target sites were amplified using extracted genomic DNA template, Platinum SuperFi Green DNA polymerase (Invitrogen), and specific primers (*SI Appendix*, Table S1). The following cycles were run: 30 s at 98 °C, followed by 33 cycles of 10 s at 98 °C; 15 s at 65 °C; 30 s at 72 °C; and 10 min at 72 °C. The PCR products were purified using the GeneJET PCR Purification Kit (Thermo Scientific). Then, 400 ng purified PCR products were hybridized in NEBuffer 2 (New England Biolabs) by heating to 95 °C for 5 min, followed by a 2 °C/second ramp down to 85 °C and a 0.1 °C/second ramp down to 25 °C on a AppliedBiosystems PCR system (Thermo Fisher Scientific). The annealed samples were digested by T7 Endonuclease I (New England Biolabs) at 37 °C for 15 min, followed by incubating at 65 °C for 5 min to stop the reaction. The products were further purified and run on a 4 to 20% Novex Tris/borate/ethylenediaminetetraacetic acid (EDTA) (TBE) gel (Invitrogen).

Statistical Analysis. Data were expressed as mean ± SD. All data were analyzed using Graphpad Prism software. The statistical difference was analyzed by one-way ANOVA. $P < 0.05$ was considered significant; $P < 0.01$ and $P < 0.001$ were considered highly significant.

Data Availability. All study data are included in the article and/or *SI Appendix*.

ACKNOWLEDGMENTS. This research was supported by UG3 TR002636-01, 5U24HG010423-02, and the NIH Research Infrastructure Grant NIH S10 OD021624.

1. F. J. Raal *et al.*; ORION-9 Investigators, Inclisiran for the treatment of heterozygous familial hypercholesterolemia. *N. Engl. J. Med.* **382**, 1520–1530 (2020).
2. K. K. Ray *et al.*; ORION-10 and ORION-11 Investigators, Two phase 3 trials of inclisiran in patients with elevated LDL cholesterol. *N. Engl. J. Med.* **382**, 1507–1519 (2020).
3. R. Koishi *et al.*, Angptl3 regulates lipid metabolism in mice. *Nat. Genet.* **30**, 151–157 (2002).
4. S. Romeo *et al.*, Rare loss-of-function mutations in ANGPTL family members contribute to plasma triglyceride levels in humans. *J. Clin. Invest.* **119**, 70–79 (2009).

5. P. Tarugi, S. Bertolini, S. Calandra, Angiopoietin-like protein 3 (ANGPTL3) deficiency and familial combined hypolipidemia. *J. Biomed. Res.* **33**, 73–81 (2019).
6. N. O. Stitziel *et al*.; PROMIS and Myocardial Infarction Genetics Consortium Investigators, ANGPTL3 deficiency and protection against coronary artery disease. *J. Am. Coll. Cardiol.* **69**, 2054–2063 (2017).
7. K. Musunuru, S. Kathiresan, Cardiovascular endocrinology: Is ANGPTL3 the next PCSK9? *Nat. Rev. Endocrinol.* **13**, 503–504 (2017).
8. F. E. Dewey *et al*., Genetic and pharmacologic inactivation of ANGPTL3 and cardiovascular disease. *N. Engl. J. Med.* **377**, 211–221 (2017).
9. Z. Ahmad *et al*., Inhibition of angiopoietin-like protein 3 with a monoclonal antibody reduces triglycerides in hypertriglyceridemia. *Circulation* **140**, 470–486 (2019).
10. M. J. Graham *et al*., Cardiovascular and metabolic effects of ANGPTL3 antisense oligonucleotides. *N. Engl. J. Med.* **377**, 222–232 (2017).
11. J. A. Doudna, The promise and challenge of therapeutic genome editing. *Nature* **578**, 229–236 (2020).
12. F. Zhang, Development of CRISPR-Cas systems for genome editing and beyond. *Q. Rev. Biophys.* **52**, 31 (2019).
13. P. D. Hsu, E. S. Lander, F. Zhang, Development and applications of CRISPR-Cas9 for genome engineering. *Cell* **157**, 1262–1278 (2014).
14. J. A. Doudna, E. Charpentier, Genome editing. The new frontier of genome engineering with CRISPR-Cas9. *Science* **346**, 1258096 (2014).
15. A. C. Chadwick, N. H. Evitt, W. Lv, K. Musunuru, Reduced blood lipid levels with in vivo CRISPR-Cas9 base editing of ANGPTL3. *Circulation* **137**, 975–977 (2018).
16. X. Chen, M. A. Gonçalves, Engineered viruses as genome editing devices. *Mol. Ther.* **24**, 447–457 (2016).
17. Z. Glass, M. Lee, Y. Li, Q. Xu, Engineering the delivery system for CRISPR-based genome editing. *Trends Biotechnol.* **36**, 173–185 (2018).
18. H. Yin *et al*., Non-viral vectors for gene-based therapy. *Nat. Rev. Genet.* **15**, 541–555 (2014).
19. M. Wang, Z. A. Glass, Q. Xu, Non-viral delivery of genome-editing nucleases for gene therapy. *Gene Ther.* **24**, 144–150 (2017).
20. M. Qiu, Z. Glass, Q. Xu, Nonviral nanoparticles for CRISPR-based genome editing: Is it just a simple adaption of what have been developed for nucleic acid delivery? *Biomacromolecules* **20**, 3333–3339 (2019).
21. M. Wang *et al*., Efficient delivery of genome-editing proteins using bioreducible lipid nanoparticles. *Proc. Natl. Acad. Sci. U.S.A.* **113**, 2868–2873 (2016).
22. J. D. Finn *et al*., A single administration of CRISPR/Cas9 lipid nanoparticles achieves robust and persistent in vivo genome editing. *Cell Rep.* **22**, 2227–2235 (2018).
23. C. Jiang *et al*., A non-viral CRISPR/Cas9 delivery system for therapeutically targeting HBV DNA and pcsk9 in vivo. *Cell Res.* **27**, 440–443 (2017).
24. J. B. Miller *et al*., Non-viral CRISPR/Cas gene editing in vitro and in vivo enabled by synthetic nanoparticle co-delivery of Cas9 mRNA and sgRNA. *Angew. Chem. Int. Ed. Engl.* **56**, 1059–1063 (2017).
25. Q. Cheng *et al*., Selective organ targeting (SORT) nanoparticles for tissue-specific mRNA delivery and CRISPR-Cas gene editing. *Nat. Nanotechnol.* **15**, 313–320 (2020).
26. J. Liu *et al*., Fast and efficient CRISPR/Cas9 genome editing in vivo enabled by bioreducible lipid and messenger RNA nanoparticles. *Adv. Mater.* **31**, e1902575 (2019).
27. A. Akinc *et al*., The Onpattro story and the clinical translation of nanomedicines containing nucleic acid-based drugs. *Nat. Nanotechnol.* **14**, 1084–1087 (2019).
28. M. Wang *et al*., Enhanced intracellular siRNA delivery using bioreducible lipid-like nanoparticles. *Adv. Healthc. Mater.* **3**, 1398–1403 (2014).
29. M. Sedic *et al*., Safety evaluation of lipid nanoparticle-formulated modified mRNA in the Sprague-Dawley rat and cynomolgus monkey. *Vet. Pathol.* **55**, 341–354 (2018).
30. K. J. Kauffman *et al*., Optimization of lipid nanoparticle formulations for mRNA delivery in vivo with fractional factorial and definitive screening designs. *Nano Lett.* **15**, 7300–7306 (2015).
31. D. Zhi *et al*., Transfection efficiency of cationic lipids with different hydrophobic domains in gene delivery. *Bioconjug. Chem.* **21**, 563–577 (2010).
32. M. Wang, S. Sun, K. A. Alberti, Q. Xu, A combinatorial library of unsaturated lipidoids for efficient intracellular gene delivery. *ACS Synth. Biol.* **1**, 403–407 (2012).
33. L. Madisen *et al*., A robust and high-throughput Cre reporting and characterization system for the whole mouse brain. *Nat. Neurosci.* **13**, 133–140 (2010).
34. M. Tabebordbar *et al*., In vivo gene editing in dystrophic mouse muscle and muscle stem cells. *Science* **351**, 407–411 (2016).
35. R. J. Platt *et al*., CRISPR-Cas9 knockin mice for genome editing and cancer modeling. *Cell* **159**, 440–455 (2014).
36. S. Tong, B. Moyo, C. M. Lee, K. Leong, G. Bao, Engineered materials for in vivo delivery of genome-editing machinery. *Nat. Rev. Mater.* **4**, 726–737 (2019).
37. A. C. Komor, A. H. Badran, D. R. Liu, CRISPR-based technologies for the manipulation of eukaryotic genomes. *Cell* **168**, 20–36 (2017).
38. X. Liang *et al*., Rapid and highly efficient mammalian cell engineering via Cas9 protein transfection. *J. Biotechnol.* **208**, 44–53 (2015).
39. S. Sabnis *et al*., A novel amino lipid series for mRNA delivery: Improved endosomal escape and sustained pharmacology and safety in non-human primates. *Mol. Ther.* **26**, 1509–1519 (2018).
40. X. Hou *et al*., Vitamin lipid nanoparticles enable adoptive macrophage transfer for the treatment of multidrug-resistant bacterial sepsis. *Nat. Nanotechnol.* **15**, 41–46 (2020).
41. B. Li *et al*., An orthogonal array optimization of lipid-like nanoparticles for mRNA delivery in vivo. *Nano Lett.* **15**, 8099–8107 (2015).
42. A. W. Duncan, C. Dorrell, M. Grompe, Stem cells and liver regeneration. *Gastroenterology* **137**, 466–481 (2009).
43. P. G. G. Chu, S. Ishizawa, E. Wu, L. M. Weiss, Hepatocyte antigen as a marker of hepatocellular carcinoma: An immunohistochemical comparison to carcinoembryonic antigen, CD10, and alpha-fetoprotein. *Am. J. Surg. Pathol.* **26**, 978–988 (2002).
44. S. Bae, J. Park, J. S. Kim, Cas-OFFinder: A fast and versatile algorithm that searches for potential off-target sites of Cas9 RNA-guided endonucleases. *Bioinformatics* **30**, 1473–1475 (2014).
45. J. L. Schmid-Burgk *et al*., OutKnocker: A web tool for rapid and simple genotyping of designer nuclease edited cell lines. *Genome Res.* **24**, 1719–1723 (2014).